

THE FAILURE ANALYSIS OF BOLTED REPAIR ON COMPOSITE LAMINATE

SHIUH-CHUAN HER and DONG-LIN SHIE

Department of Mechanical Engineering, Yuan-Ze Institute of Technology, 135,
Yuan-tung Road, Chung-Li, Tao-Yuan Shian, Taiwan, 320, Republic of China

(Received 8 August 1995; in revised form 19 May 1997)

Abstract—The bolted repair of composite laminates is analyzed based on the assumptions of rigid bolts and compatible deformation between laminate and patch. The loads transmitted to the external patches through the bolts are determined and transferred to a cosine distribution loading applied on each bolt hole. The finite element method is used to obtain the stress distribution in the laminate. The Yamada failure criteria combined with characteristic curve are employed to determine the strength and failure mode of the damaged composite laminate after the bolted repair. The results are presented for different arrangements of bolts and patch materials, to evaluate the method of bolted repair on composite laminate. © 1998 Elsevier Science Ltd.

1. INTRODUCTION

Among the major advantages of laminated composite structures over conventional metal structures are their comparatively high strength to weight, and stiffness to weight, ratios. Aeronautic structures which are sensitive to the weight, might be the best applications for composites. Since the laminated composites are vulnerable to the impact, the unexpected damage caused by an accidental impact occurs very often. Thus, composite repair becomes an important technology to reinforce the strength of the damaged composites.

In accordance with Hoskin and Baker (1987) and Brown (1985), the methods of composite repair include: flush repair, bonded repair and bolted repair. Much of the analytical work in the literature relating to composite repair has viewed the bonded repairs, while less attention has been paid to the bolted repair. The technique of bolted repair is relatively simple in comparison with bonded repairs which require perishable patching compounds, complex patching equipment, and careful surface preparation. Thus, the bolted repair may be the better choice when the fast repair is required or in the field repair where less equipments are available.

The effect of bolted repair is based on the transmission of loadings through the external patches via the bolts. The reactions of the loads are applied to each bolt hole, and simulated by a normal cosine distribution. The method has been proven good for isotropic bolt bearing specimens. Recently, the method is widely applied to simulate the lap joint for anisotropic bolt bearing specimens by many researchers.

Waszczak and Cruse (1971), De Jong (1977) and Chang *et al.* (1982, 1984) applied the normal cosine distribution on the bolt hole to determine the stress distribution and failure mode. Chang *et al.* (1984) and Agarwal (1980) assumed zero radial displacements on the half circumference of the hole. Yoshifumi and Wilson (1986) compared three different models of load applied on the bolt hole, found that the normal cosine distribution was an acceptable approach. In this investigation, the normal cosine distribution has been employed as the traction boundary condition on the bolt hole.

The bolt hole under tensile load generally fails in three basic modes referred to as tension, shearout and bearing modes. The type of damage resulting from each of these modes is illustrated in Fig. 1. Waszczak and Cruse (1971) predicted the lamina failure by the distortional energy failure criterion. This criterion was sufficient to predict the failure

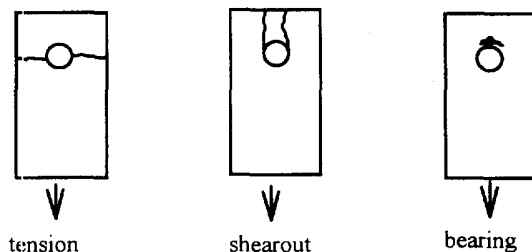


Fig. 1. Three basic failure modes.

modes in all but the shearout cases. The average stress failure criterion was used to predict the failure load and mode by Agarwal (1980). In some cases, the magnitude of the predicted failure load differs by approximately 50% from experimental data. Chang and Scott (1982) analyzed the failure of the bolt hole by the characteristic curve in conjunction with the Yamada failure criteria. By comparing with the experimental data, Yamada failure criteria is shown to be a better method in predicting the failure of the bolt hole.

2. PROBLEM STATEMENT

As the damage occurs, the strength of the composite laminate is decreased. In order to reinforce the strength of the laminate, external patches are attached to the damaged area. The bearing load across the damaged area is reduced by transmitting parts of the load through the patches. The effect of the bolted repair in reducing the load across the damaged area is investigated in this paper. To simplify the study, the damaged area is simulated as a hole.

Consider a composite laminate with a damaged area of radius R , two external patches are bolted on the top and bottom to repair the damaged laminate. A tensile load P is applied to the laminate as shown in Fig. 2.

In this study the analysis of bolted repair on composite laminate is based on the following assumptions:

- (1) The bolts are regarded as a rigid body and zero clearance between holes and bolts.
- (2) The deformations of the damaged laminate and external patches are the same between two neighboring bolts.
- (3) The loads applied to the bolts and bolt holes follow a normal cosine distribution.
- (4) The arrangement of bolts are symmetric with respect to the centerline.
- (5) The effect of the friction on the bolts and clamping pressure is ignored.

To avoid bending effect, the layup of the lamina and load are symmetric with respect to the middle plane. Therefore, the analysis may be simplified to a two-dimensional model.

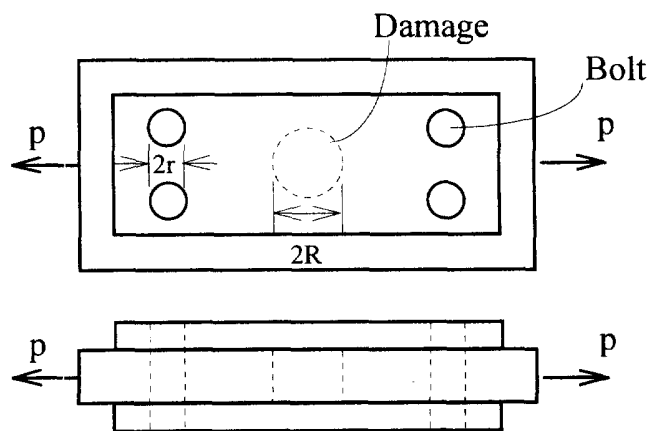


Fig. 2. Model of the bolted repair.

3. PROCEDURES OF ANALYSIS

3.1. *Effective engineering constants*

In the case of symmetric laminates, bending can be decoupled from the in-plane loads. The membrane strain–stress relations from Tsai and Hahn (1980) are as follows:

$$\begin{Bmatrix} \varepsilon_1^0 \\ \varepsilon_2^0 \\ \varepsilon_6^0 \end{Bmatrix} = \begin{bmatrix} a_{11} & a_{12} & a_{16} \\ a_{21} & a_{22} & a_{26} \\ a_{61} & a_{62} & a_{66} \end{bmatrix} \begin{Bmatrix} N_1 \\ N_2 \\ N_6 \end{Bmatrix} \quad (1)$$

where $N_i = \sigma_i \cdot t$, and t is the thickness of the laminate.

One can calculate the effective engineering constants of the laminate from the compliance matrix as follows:

in-plane longitudinal modulus

$$E_1^0 = \frac{1}{a_{11}t}$$

in-plane transverse modulus

$$E_2^0 = \frac{1}{a_{22}t}$$

in-plane shear modulus

$$E_6^0 = \frac{1}{a_{66}t}$$

in-plane Poisson's ratio

$$\nu_{21}^0 = -\frac{a_{12}}{a_{11}}$$

in-plane shear coupling coefficient

$$\nu_{61}^0 = \frac{a_{61}}{a_{11}}$$

in-plane normal coupling coefficient

$$\nu_{16}^0 = \frac{a_{16}}{a_{66}}. \quad (2)$$

3.2. *Calculate the load on the bolts*

The loads acting on the bolt can be divided into two parts:

- (1) In the middle section, results from the reaction force by the laminate.
- (2) On the top and bottom, result from the reaction forces by the external patches.

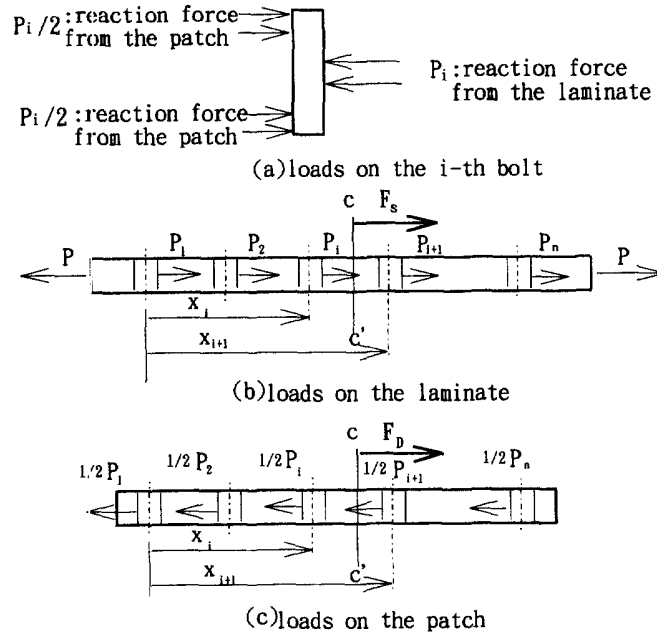


Fig. 3. Free body diagram of the bolted repair.

Figure 3(a) shows the free-body diagram of the i -th bolt. The force F_s acting on the cross-section cc' (between i th and $(i+1)$ th bolts) of the laminate as shown in Fig. 3(b) is expressed as

$$F_s = P - P_1 - P_2 - \dots - P_i = P - \sum_{k=1}^i P_k \quad x_i \leq x \leq x_{i+1}$$

where P is the applied load and P_k is the load on k th bolt hole.

The strain in the cross-section cc' of the laminate is

$$\varepsilon_s = \frac{\sigma_s}{E_s} = \frac{F_s}{E_s A_s} = \frac{dl_s}{dx}$$

where $E_s(x)$, $A_s(x)$ represent the effective longitudinal modulus and the cross-section area of the laminate, respectively, and σ_s , $\varepsilon_s(x)$, $dl_s(x)$ represent the stress, strain and displacement of the laminate in the longitudinal direction, respectively.

Thus

$$dl_s(x) = \frac{P - \sum_{k=1}^i P_k}{E_s(x) A_s(x)} dx, \quad x_i \leq x \leq x_{i+1}. \quad (3)$$

The force F_D acting on the cross-section cc' of the external patch, as shown in Fig. 3(c), is

$$F_D = \frac{1}{2} P_1 + \frac{1}{2} P_2 + \dots + \frac{1}{2} P_i = \frac{1}{2} \sum_{k=1}^i P_k \quad x_i \leq x \leq x_{i+1}.$$

The strain in the cross-section cc' of the external patches is

$$\epsilon_D = \frac{\sigma_D}{E_D} = \frac{F_D}{E_D A_D} = \frac{dl_D}{dx}$$

where $E_D(x)$, $A_D(x)$ represent the effective longitudinal modulus and the cross-section area of the external patches, respectively, and σ_D , $\epsilon_D(x)$, $dl_D(x)$ represent the stress, strain and displacement of the external patches in the longitudinal direction, respectively.

So

$$dl_D(x) = \frac{\frac{1}{2} \sum_{k=1}^i P_k}{E_D(x)A_D(x)} dx, \quad x_i \leq x \leq x_{i+1}. \tag{4}$$

Utilizing the compatible deformations between laminate and external patches yields

$$\int dl_s(i, i+1) = \int dl_D(i, i+1). \tag{5}$$

Substituting eqns (3) and (4) into eqn (5), results in

$$\sum_{k=1}^i P_k = \frac{P}{1 + \frac{f_D}{2f_s}} \quad (i = 1, 2, \dots, n-1) \tag{6}$$

where

$$f_s = \int_{x_i}^{x_{i+1}} \frac{dx}{E_s(x)A_s(x)}, \quad f_D = \int_{x_i}^{x_{i+1}} \frac{dx}{E_d(x)A_d(x)}$$

are the flexibility of the laminate and external patches, respectively.

The overall equilibrium of the laminate shown in Fig. 3(b) leads to

$$\sum_{k=1}^n P_k = 0. \tag{7}$$

Equations (6) and (7) give a total of n equations, and are able to solve the unknown force P_k acted on each bolt.

3.3. The flexibility of the plate with a hole

Equation (6) involves the flexibility of the laminate (f_s) and patches (f_D). To calculate the flexibility, consider the plate (width W_0 , thickness t) with a hole (radius r) as shown in Fig. 4. The area of the cross-section cc' can be written as $A(x) = tW(x)$.

If x is outside the region of the hole

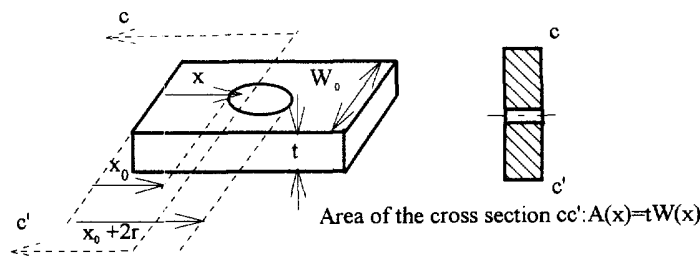


Fig. 4. Cross-section of a plate.

$$W(x) = W_0.$$

If x is inside the region of the hole

$$W(x) = W_0 - 2\sqrt{r^2 - (r + x_0 - x)^2}, \quad x_0 \leq x \leq x_0 + r$$

$$W(x) = W_0 - 2\sqrt{r^2 - (x - x_0 - r)^2}, \quad x_0 + r \leq x \leq x_0 + 2r.$$

The flexibility of the plate is

$$f = \int_{x_i}^{x_{i+1}} \frac{dx}{E(x)A(x)} = \frac{1}{Et} \int_{x_i}^{x_{i+1}} \frac{dx}{W(x)}. \quad (8)$$

3.4. The normal cosine distribution

From the previous derivations one obtains the load (P_i) acting on each bolt. The reaction of the load is then transferred to a normal cosine distribution on the half circumference of the hole as shown in Fig. 5, and is expressed as

$$T(\theta) = T_{\max} \cos \theta. \quad (9)$$

The resultant of the distribution forces in the loading axis is equal to P_i , thus

$$\int_{-\pi/2}^{\pi/2} T(\theta) \cos \theta t r d\theta = P_i \quad (10)$$

where r is the radius of the bolt and t is the thickness of the plate.

Substituting eqn (9) and eqn (10) yields

$$T_{\max} = \frac{2P_i}{\pi t r}.$$

The normal cosine distribution forces can be considered as the traction boundary condition on the bolt holes of the laminate and external patches.

3.5. Finite element analysis

For a symmetric layup of composite laminate under the in-plane loading, the bending effect can be neglected. In this study, the applied loads are parallel to the plate and are symmetric with respect to the middle plane. A two-dimensional model was adopted in the

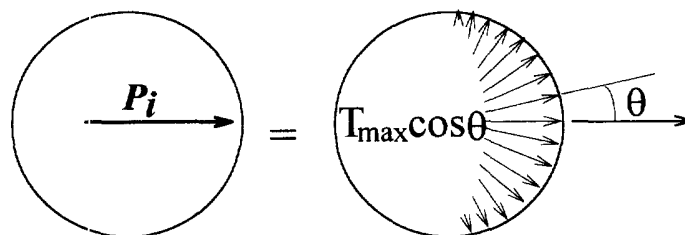


Fig. 5. Normal cosine distribution.

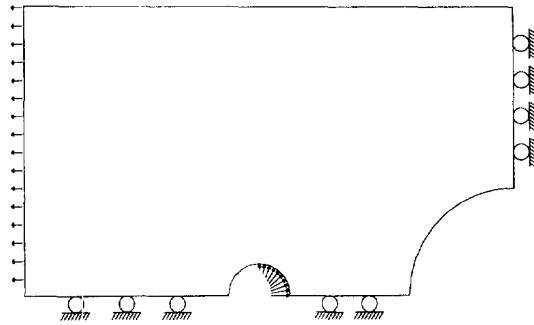


Fig. 6. Boundary condition of finite element model.

analysis. The finite element method was employed in the numerical analysis. A typical two-bolt repair model is shown in Fig. 6, due to the symmetric conditions only one quarter of the entire model is required.

4. PREDICTION OF FAILURE

4.1. Calculate the stresses of the each ply

The strains and stresses computed from the finite element method are for the effective laminate. The strains in each ply are assumed to be the same as the effective laminate. Thus, one can express the strains of each ply in the coordinate system coincided with the fiber direction as follows :

$$\begin{Bmatrix} \varepsilon_x \\ \varepsilon_y \\ \varepsilon_s \end{Bmatrix} = \begin{Bmatrix} c^2 & s^2 & cs \\ s^2 & c^2 & -cs \\ -2cs & 2cs & c^2 - s^2 \end{Bmatrix} \begin{Bmatrix} \varepsilon_1 \\ \varepsilon_2 \\ \varepsilon_6 \end{Bmatrix} \tag{11}$$

where $c = \cos \theta$, $s = \sin \theta$, $\varepsilon_1, \varepsilon_2, \varepsilon_6$ are the strains of the effective laminate, $\varepsilon_x, \varepsilon_y, \varepsilon_s$ are the strains of each ply in the coordinate system with x -axis directed along the fiber direction, and θ is the angle between the global x -axis and the fiber direction.

The stresses of each ply are determined by the following relations

$$\begin{Bmatrix} \sigma_x \\ \sigma_y \\ \sigma_s \end{Bmatrix} = \begin{Bmatrix} Q_{xx} & Q_{xy} & 0 \\ Q_{xy} & Q_{yy} & 0 \\ 0 & 0 & Q_{ss} \end{Bmatrix} \begin{Bmatrix} \varepsilon_x \\ \varepsilon_y \\ \varepsilon_s \end{Bmatrix}$$

$$Q_{xx} = \frac{E_x}{(1 - v_{xy}v_{yx})}, \quad Q_{yy} = \frac{E_y}{(1 - v_{xy}v_{yx})}$$

$$Q_{xy} = v_{xy}E_x(1 - v_{xy}v_{yx}), \quad Q_{ss} = G_{xy} \tag{12}$$

4.2. Characteristic curve and failure criterion

4.2.1. *Yamada's criteria* (1978). This criterion is based on the assumption that just prior to failure of the laminate every ply has failed due to cracks along the fiber. It states that failure occurs when the following condition is met in any one of the plies :

$$\left(\frac{\sigma_{xi}}{X}\right)^2 + \left(\frac{\sigma_{xyi}}{S_c}\right)^2 = e^2 \begin{cases} e < 1, & \text{no failure} \\ e \geq 1, & \text{failure} \end{cases} \tag{13}$$

where σ_{xi} is the longitudinal stress in i th ply, σ_{xyi} is the shear stresses i th ply, X is the

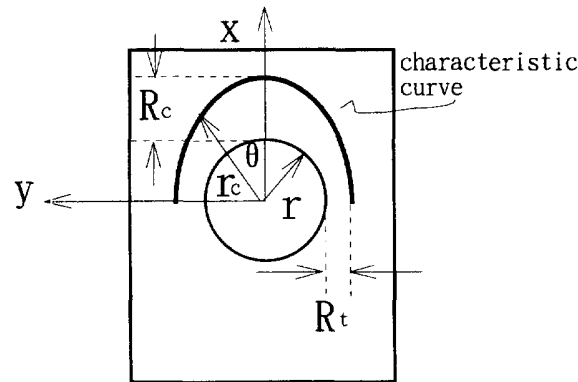


Fig. 7. Characteristic curve.

longitudinal tensile strength of a ply, S_c is the shear strength of the laminate. As indicated in eqn (13) failure occurs when e is equal to or greater than unity.

4.2.2. *Characteristic curve.* Chang (1982) proposes that failure occurs when in any one of the plies the combined stresses satisfy an appropriately chosen failure criterion at any point on a characteristic curve. The characteristic curve (Fig. 7) is specified by the expression

$$r_c = r + R_t + (R_c - R_t) \cos \theta, \quad -\frac{\pi}{2} \leq \theta \leq \frac{\pi}{2} \quad (14)$$

where R_c and R_t are the characteristic lengths for tension and compression, respectively. These parameters can be determined experimentally by measuring the tensile and compressive strengths of notched laminates. R_c and R_t depend only on the material.

In this investigation, the stresses in the characteristic curve equation (14) are substituted into Yamada failure criterion equation (13) to determine the value of e . Failure occurs when the parameter e is equal to or greater than unity at any point on the characteristic curve.

4.3. Prediction of failure load and failure mode

4.3.1. *Failure load.* According to the linear elastic theory, the stress fields are linearly proportional to the applied load P . Thus, the failure load P_{\max} can be determined from the following relation:

$$P_{\max} = \frac{P}{e_0} \quad (15)$$

where P is the applied load and e_0 is the maximum value of e on the characteristic curve under the applied load P .

4.3.2. *Failure mode.* The failure mode is dependent upon the location θ_f on the characteristic curve (as shown in Fig. 7) where the maximum value of e is occurred. In general, the failure modes are characterized to the following three types (Chang, 1982):

$$\begin{aligned} -15^\circ < \theta_f < 15^\circ & \text{ bearing mode,} \\ 30^\circ < \theta_f < 60^\circ & \text{ shearout mode,} \\ 75^\circ < \theta_f < 90^\circ & \text{ tension mode.} \end{aligned} \quad (16)$$

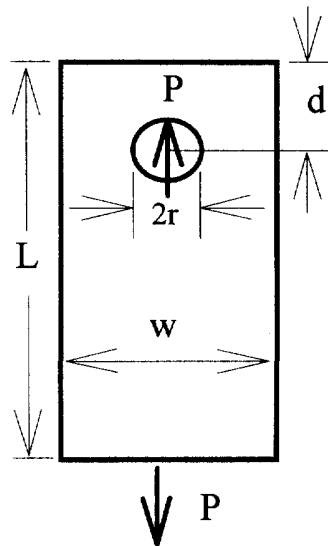


Fig. 8. Plate with a loaded hole.

5. RESULTS

5.1. Comparison of the literatures

One numerical example has been solved to examine the accuracy of the finite element software ANSYS before the actually bolted repair analysis. Consider a plate containing a hole subjected to loads P on the hole and bottom edge as shown in Fig. 8 the associated dimensions are as follows:

edge distance: $d = 30.48$ mm,
 radius of the bolt: $r = 3.81$ mm,
 width: $W = 60.96$ mm,
 length: $L = 106.68$ mm.

The load P on the hole is transferred to a cosine distribution as derived in eqn (10) and becomes the traction boundary condition on the hole. The numerical analysis has been carried out by the ANSYS finite element software. The stress concentration factor (SCF) around the hole is defined by

$$\text{SCF} = \frac{(\sigma_{xx})_{\max}}{\sigma_b}$$

where $(\sigma_{xx})_{\max}$ is the maximum stress in the plate and σ_b is the average stress over the area of the bolt hole

$$\sigma_b = \frac{P}{t2r}$$

Table 1 shows the stress concentration factors on the loaded hole between present

Table 1. S.C.F. on the loaded hole
(Chang *et al.* 1982)

Investigators	S.C.F.
Present result	0.931
Chang Fu-Kuo	0.985
Hong	0.955
DeJong	1.058
Eshwar <i>et al.</i>	0.922

Table 2. Material and dimensions of single bolt joint laminate

Case no.	T300/SP286 Layup	2r (mm)	W/2r	d/2r	L/2r	H(thickness) (mm)
1	[0/±45/90] _s	4.76	5.336	2.983	14.68	1.067
2	[0/±45/90] _s	4.76	8.025	4.013	14.68	1.067
3	[0/90] _{2s}	4.76	5.336	2.983	14.68	1.118

Table 3. Failure load and mode of the single bolt joint laminate

Case no.	Experimental results		Predicting results			Percent difference (%)
	Failure mode	Failure load P_o (N) (Agarwal)	Failure mode	Failure load P_c (N) (Chang)	Failure load P_A (N) (present)	
1	tension	4982	tension	5413.5	5739.0	5.26
2	bearing	5204	bearing	5711.4	6115.3	6.57
3	shearout	3002	shearout	3371.3	3455.6	7.46

result and other researchers, the good agreement among these results demonstrate the accuracy of the finite element model.

The same geometry as shown in Fig. 8 is used to solve the single bolt joint for composite laminate by Agarwal (1980) and Chang (1982). Three different layups and associated dimensions are shown in Table 2. These are chosen as examples of examining the failure load and mode on the bolt hole. Utilizing the method described in the previous sections, the failure load and mode can be obtained. The results are shown in Table 3 which contains experimental results from Agarwal (1980), numerical results from Chang (1982) and present results. Good correlation among these results indicate that present method is reliable in predicting the failure load and mode around the holes.

5.2. Examples

In the following bolted repair analysis, the damaged laminate (length $L = 160$ mm, width $W = 80$ mm, thickness $t = 2$ mm) is repaired by two external patches (length 100 mm, width 50 mm, thickness 1 mm) the radius of bolts is 3 mm and the damaged area is simulated by a hole with radius of 12 mm. The characteristic length R_{oc} and R_{io} for graphite/epoxy T300/5208 are 2.032 mm and 0.457 mm, respectively, according to Wan and Chang (1992). The plate is subjected to a uniform tensile stress σ_o ($\sigma_o P / (W \cdot t)$) along the two edges as shown in Fig. 2.

In order to understand the efficiency of the bolted repair four parameters, which are considered to be important in the bolted repair, have been studied in this investigation.

- (1) Plate materials: composite laminate T300/5208 (material properties shown in Table 4).
- (2) Patch materials: aluminum alloy, titanium alloy or T300/5208 $[0_2/(\pm 30)_2/90_2]_s$ (material properties shown in Table 4).

Table 4. Material properties

Material no.	Material	E_x (GPa)	E_y (GPa)	ν_x	G_s (GPa)
1	Al alloy 2024 T3	72	72	0.32	27
2	Ti alloy 6 Al/4v	110	110	0.31	41
3	Composite T300/5208	181	10.3	0.28	7.17

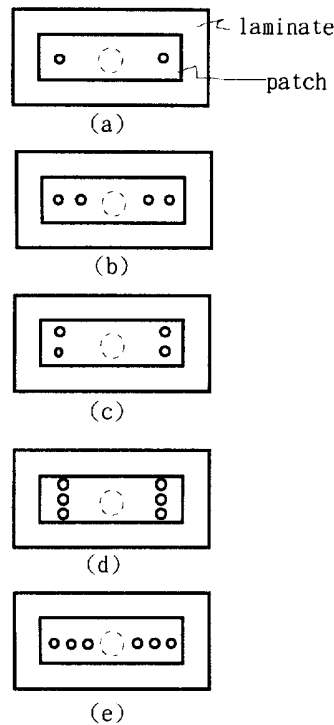


Fig. 9. Arrangement of bolts.

- (3) Number of bolts : 2, 4 or 6 bolts (as shown in Fig. 9).
- (4) Arrangement of bolts : parallel or perpendicular to the loading direction (as shown in Fig. 9).

Based on these four parameters, three groups of 15 different combinations of repair models have been established as shown in Table 5.

In group A, the damaged plate is a laminate with layup $[0_2/(\pm 30)_2/90_2]_s$, and the external patches are aluminum alloy. The failure load of the damaged laminate before the bolted repair is 39174N. The failure load and mode after the bolted repair are shown in Table 7. In all cases, the failure is initiated from the bolt hole instead of the damaged hole,

Table 5. Bolted repair model

Repair model	Material no. (Table 4)		Bolts no.	Arrangement of bolts
	Plate	Patch		
A1	3	1	2	Fig. 9(a)
A2	3	1	4	Fig. 9(b)
A3	3	1	4	Fig. 9(c)
A4	3	1	6	Fig. 9(d)
A5	3	1	6	Fig. 9(e)
B1	3	2	2	Fig. 9(a)
B2	3	2	4	Fig. 9(b)
B3	3	2	4	Fig. 9(c)
B4	3	2	6	Fig. 9(d)
B5	3	2	6	Fig. 9(e)
C1	3	3	2	Fig. 9(a)
C2	3	3	4	Fig. 9(b)
C3	3	3	4	Fig. 9(c)
C4	3	3	6	Fig. 9(d)
C5	3	3	6	Fig. 9(e)

Table 6. Load on the bolts of repaired group A

Repair model	Load on the each bolt (10^{-5} N)			Total load on the bolts	Load transmitted to patch $\frac{R}{P} \times 100\%$
	External (or upper) bolt	Middle bolt	Internal (or lower) bolt		
A1	5.45	—	—	5.45	34.07%
A2	5.01	—	0.552	5.56	34.75%
A3	2.71	—	2.71	5.43	33.94%
A4	1.80	1.80	1.80	5.39	33.68%
A5	4.98	0	0.67	5.65	35.92%

Note: applied load $P = 1.6 \times 10^{-4}$ N.

Table 7. Failure load and mode of repaired group A

Repair model	Failure location	Failure mode	Failure load after repair P_r (N)	Increase of failure load after repair $e_r = \frac{P_r - P_d}{P_d} \times 100\%$
A1	bolt hole	shearout	29868.62	decrease
A2	bolt hole	shearout	31927.55	decrease
A3	bolt hole	tension	45907.72	17.19%
A4	bolt hole	tension	48955.84	24.97%
A5	bolt hole	shearout	28917.77	decrease

Note: failure load before repair $P_d = 39174.1$ N.

these results indicate that the load across the damaged area have been substantially reduced. Table 6 shows the load transmitted by each bolt to the external patch. The bolt holes which are subjected to the reaction forces by the bolts become the critical region. Table 7 shows that only the repair models of A3 and A4 have an increase of failure load 17.19 and 24.97%, respectively. The failure load is decreased in the other repair models due to the high concentration on the bolt holes.

In group B and C, the external patches are replaced by titanium and T300/5208 $[0_2/(\pm 30)_2/90_2]_s$, respectively. Tables 8 and 10 show the loads transmitted to the external patch via the bolts. Tables 9 and 11 show the failure load and mode corresponding to each repair model. Among those models B3, B4, C3 and C4 which are able to increase the failure load are the better repair models.

The major difference among groups A, B and C is the material of patch. From Tables 6, 8 and 10, the sum of the loads on the bolts is approximate to a constant in each group, i.e. the total loads transmitted to the external patches is dependent on the material of patch, and independent of the number of bolts and arrangement of bolts. External patches with high stiffness can carry more loads and reduce loads across the damaged area, because of the assumption of the compatible deformation between plate and external patches. The

Table 8. Load on the bolts of repaired group B

Repair model	Load on the each bolt (10^{-5} N)			Total load on the bolts	Load transmitted to the patch $\frac{R}{P} \times 100\%$
	External (upper) bolt	Middle bolt	Internal (lower) bolt		
B1	7.06	—	—	7.06	44.12%
B2	6.57	—	0.611	7.18	44.86%
B3	3.52	—	3.52	7.04	43.97%
B4	2.33	2.33	2.33	6.99	43.69%
B5	6.53	0	0.74	7.27	45.45%

Note: applied load $P = 1.6 \times 10^{-4}$ N.

Table 9. Failure load and mode of repaired group B

Repair model	Failure location	Failure mode	Failure load after repair P_r (N)	Increase of failure load after repair $e_f = \frac{P_r - P_d}{P_d} \times 100\%$
B1	bolt hole	shearout	23004.65	decrease
B2	bolt hole	shearout	24366.01	decrease
B3	bolt hole	tension	42381.18	8.19%
B4	bolt hole	tension	47202.70	20.49%
B5	bolt hole	shearout	21879.99	decrease

Note: failure load before repair: $P_d = 39174.1$ N.

Table 10. Load on the bolts of repaired group C

Repair model	Load on the each bolt (10^{-5} N)				Total load on the bolts	Load transmitted to the patch $\frac{R}{P} \times 100\%$
	External (or upper) bolt	Middle bolt	Internal (or lower) bolt			
C1	4.727	—	—	4.727	29.54%	
C2	4.314	—	0.513	4.827	30.17%	
C3	2.353	—	2.353	4.706	29.41%	
C4	1.599	1.599	1.599	4.676	29.23%	
C5	4.296	0	0.618	4.914	30.71%	

Note: applied load $P = 1.6 \times 10^{-4}$ N.

Table 11. Failure load and mode of repaired group C

Repair model	Failure location	Failure mode	Failure load after repair P_r (N)	Increase of failure load after repair $e_f = \frac{P_r - P_d}{P_d} \times 100\%$
C1	bolt hole	shearout	37490	decrease
C2	bolt hole	tension	37700	decrease
C3	bolt hole	tension	47780	21.97%
C4	bolt hole	tension	49550	26.49%
C5	bolt hole	shearout	35360	decrease

Note: failure load before repair: $P_d = 39174.1$ N.

loads transmitted to external patches with material of aluminum, titanium and composite T300/5208 are approximate to 34, 44 and 30% of the applied load, respectively.

In general, there are two aspects to evaluate the efficiency of repair: (1) maximizing the increase of failure load, and (2) minimizing the increase of weight. Table 12 summarizes the results of efficiency in terms of failure load and weight for the repaired models shown in Table 5. By comparing these results, the repair models with composite patch have a better performance overall. C4 and 26.5% of increase of failure load and 33.5% of increase of weight is the best repair model.

6. CONCLUSIONS

From the previous numerical results, the bolted repair is good in terms of reducing the high stresses around the damaged area, but the high stress concentration around the bolt holes becomes the major disadvantage of the method of the bolted repair. To improve the method of the bolted repair and make it more reliable, the following proposals are suggested to reduce the high stresses around the bolt holes.

Table 12. Repair efficiency

Repair model	Increase of load after repair	Increase of weight after repair
	$e_f = \frac{P_r - P_d}{P_d} * 100\%$	$e_f = \frac{w_r - w_d}{w_d} * 100\%$
A1	decrease	74.2%
A2	decrease	75.7%
A3	17.2%	75.7%
A4	25%	77.3%
A5	decrease	77.3%
B1	decrease	120.3%
B2	decrease	121.2%
B3	8.2%	121.2%
E4	20.5%	122.2%
E5	decrease	122.2%
C1	decrease	42.2%
C2	decrease	35.9%
C3	22%	35.9%
C4	26.5%	33.5%
C5	decrease	33.5%

6.1. Increasing the number of bolts

The total load passing through the external patches is approximate to a constant, and is distributed among the bolts. One may expect the loading transmitted by each bolt will be reduced when the total number of bolts are increased, thereby reduce the high stresses around the bolt holes.

6.2. Improving the arrangement of the bolts

From Tables 6, 8 and 10, most of the loads transmitted to the patches is concentrated on the external bolt for the repair models of A2, A5, B2, B5, C2, C5, result of failure initiated from the external bolt hole under a smaller load. However, the load transmitted to the patches are distributed among the bolts for the repair models of A3, A4, B3, B4, C3 and C4, result of larger failure load. So one may conclude that the bolts align in the direction of perpendicular to the loading is the better arrangement of bolts.

6.3. Choosing the external patches

The load passing through the external patches is dependent on the ratio of stiffness between patch and plate. So the right choice of material for external patches could reduce the stresses on both the damaged area and bolt hole. The strength of laminates containing a hole is dependent on both the stress and the size of the hole. Although the bolted repair induces high stresses on the bolt holes, the size of bolt holes is smaller than the damaged hole. Thus, the bolted repair is still capable of reinforcing the strength of the damaged laminate.

REFERENCES

- Agarwal, B. L. (1980) Static strength prediction of bolted joints in composite material. *AIAA Journal* **18**, 1371–1375.
- Chang, F. K., Scott, R. A. and Springer, G. S. (1982) Strength of mechanically fastened composite joints. *Journal of Composite Materials* **16**, 470–493.
- Chang, F. K., Scott, R. A. and Springer, G. S. (1984) Failure of composite laminates containing pin load holes—method of solution. *Journal of Composite Materials* **18**, 255–278.
- Chang, F. K. and Scott, R. A. (1984) Failure strength of non-linearly elastic composite-laminates containing a pin loaded hole. *Journal of Composite Materials* **18**, 464–477.
- DeJong, T. (1977) Stress around pin loaded holes in elastically orthotropic or isotropic plates. *Journal of Composite Materials* **11**, 313–331.
- Brown, H. (1985) *Composite Repairs SAMPE Monograph No. 1*, SAMPE.
- Hoskin, B. C. and Baker, A. A. (1986) *Composite Material for Aircraft Structure*. AIAA.
- Tsai, S. W. and Hahn, H. T. (1980) *Introduction to Composite Material*. Technomic.

- Wan, Y. B. and Chang, C. C. (1992) *Connection of Composite Structures*. Defense Industry, Beijing, China.
- Waszczak, J. P and Cruse, T. A. (1971) Failure mode and strength prediction of anisotropic bolt bearing specimens. *Journal of Composite Materials* **5**, 421–425.
- Yamada, S. E. (1978) Analysis of laminate strength and its distribution. *Journal of Composite Materials* **12**, 275–284.
- Tsujimoto, Y. and Wilson, D. (1986) Elasto-plastic failure analysis of composite bolted joints. *Journal of Composite Materials* **20**, 236–252.